Journal of Geoscience and Environment Protection, 2020, 8, 1-16
https://www.scirp.org/journal/gep
ISSN Online: 2327-4344
ISSN Print: 2327-4336

Petro-Structural Study of Paragneiss in the SASCA Domain (Gbowé Sector at Grand-Béréby), Southwestern Côte d'Ivoire

Fossou Jean-Luc Hervé Kouadio, Mamadou Sangare, N'Guessan Nestor Houssou, Marc Ephrem Allialy, Sagbrou Chérubin Djro

Laboratory of Geology, Mineral and Energy Resources (LGRME), Faculty of Earth Science and Mineral Resources, Félix Houphouët Boigny University, Abidjan, Côte d'Ivoire
Email: fossoujean@gmail.com

How to cite this paper: Kouadio, F. J.-L. H., Sangare, M., Houssou, N. N., Allialy, M. E., & Djro, S. C. (2020). Petro-Structural Study of Paragneiss in the SASCA Domain (Gbowé Sector at Grand-Béréby), Southwestern Côte d'Ivoire. *Journal of Geoscience and Environment Protection, 8,* 1-16.
https://doi.org/10.4236/gep.2020.85001

Received: April 5, 2020
Accepted: May 3, 2020
Published: May 6, 2020

Abstract

The petrographic and structural study of Gbowé (Grand-Béréby) formations located in the SASCA domain (South-West of Côte d'Ivoire) revealed migmatitic paragneisses. For an in-depth understanding of the petrographic, structural and metamorphic characteristics, six (6) thin sections were made from these paragneisses. These gneisses are characterized by paleosomes and neosomes (leucosome and melanosome), consisting of quartz, garnet, plagioclase, biotite, cordierite, sillimanite, myrmekite and microcline. The mineralogical assemblage thus described indicates a retrograde metamorphism (transition from granulitic facies to amphibolitic facies). The structural and microstructural study identified two types of deformation (ductile and brittle). The ductile deformation is characterized by phases D1 (NE-SW flattening) and D2 (NW-SE flattening), materialized by foliations (N140˚, N050˚), folds (asymmetrical folds, similar folds, concentric folds, ptymatic folds) and boudins. Fracture schistosity and fold fracture schistosity are characteristic of the brittle deformation (phase D3). The microstructural study coupled with the metamorphic study shows that the deformations had an impact on the texture of the minerals (recrystallization and mineral reactions). It also allowed giving the paragenesis of phases D1 and D2. The D1 phase is characterized by garnet1, biotite1, quartz1, sillimanite1 and cordierite1 and the D2 phase is characterized by garnet1, quartz2, sillimanite2, biotite2, garnet2 and orthose2. These parageneses thus highlighted bear witness to a polydeformation and polymorphism that affects the study area.

Keywords

Petrography, Structural, Migmatitic Paragneiss, Retrograde Metamorphism, Gbowé, SASCA Domain, Côte d'Ivoire

1. Introduction

The geological formations of south-west Côte d'Ivoire consist of several metamorphic units, and Eburnean plutonic rocks grouped into two domains (Papon, 1973): the Man domain and the SASCA domain (named after the Sassandra and Cavally rivers which limit this area). In the Man domain, a single metamorphic unit (Toulépleu-Ity unit) with particular lithological and structural characteristics is mapped, whereas in the SASCA domain, four metamorphic units are observed (Louga-Kounoukou unit, Davo unit, Hana-Lobo unit and Monts Trou unit) composed mainly of metasediments (paragneiss, micaschists) and grey gneiss; all intruded by granitoids and dolerite (or metabasite) dykes (Papon, 1973; Kouadio, 2017). The SASCA domain is composed of an old Liberian granitic and metamorphic basement (Koffi et al., 2020, Kouamelan et al., 2018) over which birimian formations of pelitic, tuffaceous, acidic and/or basic origin have transgressed, to which the micaschists of Kounoukou are associated (Papon, 1973). This zone is also characterized by the coexistence of high and medium grade metamorphic units (Papon, 1973, Kouamelan et al., 2015; Kouadio, 2017) with the presence of Archean crustal relics (Kouamelan, 1996; Kouamelan et al., 1997a, 2015, Petersson et al., 2016, 2017). Geochemical studies carried out in the SASCA domain show that most of the metasediments in this zone correspond to grauwackes (Papon, 1973). Recent SASCA studies on paragneisses in the Tabou and Grand-Béréby areas indicate that they belong to the grauwackes and shales and are derived from felsic to intermediate plutonic rocks (Kouadio et al., 2016; Koffi et al., 2018). However, there is a lack of very thorough and detailed petro-structural studies in this zone. For this reason, the Gbowé sector, located in the southwestern part of Côte d'Ivoire, at Grand-Béréby, is the subject of our study. The geological formations in this sector raise several questions, namely: 1) What are the petrographic characteristics of the main formations encountered?, 2) What are the deformations and metamorphisms that have affected these formations and their relative chronology? and 3) How can we explain the formation of these formations?

This study is a contribution to a better understanding of the petrography and structural features of Grand-Béréby, more specifically those of the Gbowé sector.

2. Geological Context

Côte d'Ivoire belongs to the West-African craton stabilized since 1.9 Ga. It lies precisely on the Leo's ridge. Based on new geochronological data published by Boher et al., (1992); Kouamelan, (1996); Kouamelan et al., (1997b) and Doumbia (1998), Côte d'Ivoire is made up of four geological domains (**Figure 1**) including the Archean Domain (located West of the Sassandra fault), the Transition Domain

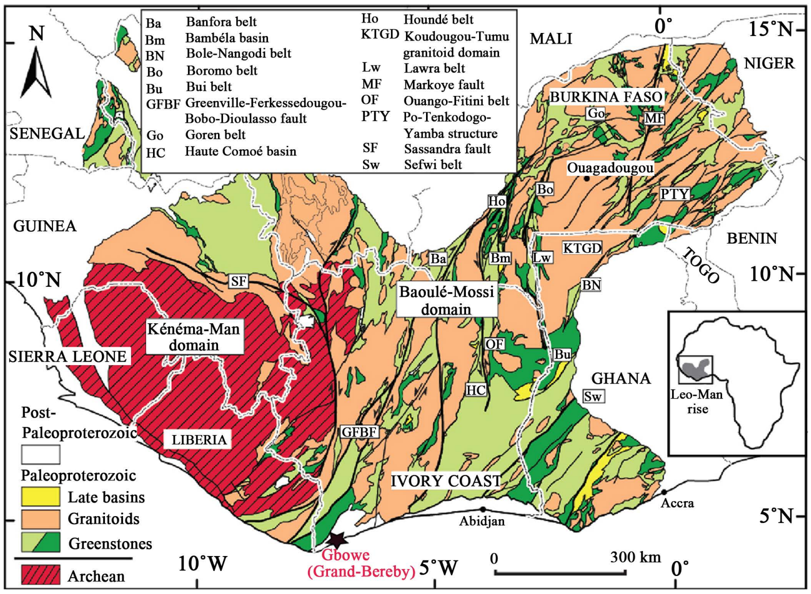

Figure 1. Simplified geological map of the West African craton, and the location of study area Gbowé sector (Grand-Béréby). Modified map SIG Afrique by BRGM, Milesi et al., 2004.

(transition from Archean to Birimian), the Paleoproterozoic Domain (or Birimian Domain located East of the Sassandra fault) and the Sedimentary Basin (located in the Southern part of the country). The Archean domain, also known as the Kenema-Man domain, is an Archean core consisting mainly of tonalitic grey gneisses, banded magnetite quartzites and biotite migmatites (Camil, 1984; Thieblemont et al., 2004, Koffi et al., 2020). The Proterozoic or Baoulé-Mossi domain is characterized by formations affected by Eburnean orogeny (2.1 ± 0.1 Ga) (Arnould, 1961; Bonhomme, 1962, Gasquet et al., 2003, Pouclet et al., 2006; Vidal et al., 2009). It is possible to group the lithologies in this domain into a few families. These are the family of tholeiitic basaltic green rocks and associated plutonic rocks, the family of calc-alkaline rocks, the family of extensive granodioritic to granitic batholiths and the family of detrital metasedimentary rocks. The transition zone or SASCA domain is characterized by the contamination of juvenile Birimian formations by Archean crust (intermediate Nd model age and inherited zircons). The presence of inherited zircons with Pb/Pb isotopic ages made by direct evaporation of 3132 ± 9 Ma and 3141 ± 2 Ma, respectively, proves the existence of Archean rock segments into the Birimian (Kouamelan, 1996; Kouadio et al., 2016). The sedimentary basin extends along the Atlantic coast, which represents the country's natural Southern border. Its history is linked to that of Gondwana breakup and the opening of the South Atlantic in the Lower Cretaceous (Blarez, 1986). This opening led to the separation of Africa and South America.

3. Methodology

This work was carried out in two main stages, namely the field stage and the laboratory stage. Respective methods for each of these steps have been developed.

3.1. Macroscopic Petrography and Structural Analysis

Both of these processes took place on the field after the study site had been delineated. Macroscopic petrography made it possible to identify the lithological facies present on the site by observing the petrographic units with the naked eye and/or magnifying glass. This identification was made basing on the criteria of macroscopic description of the rocks. The structural analysis made it possible to identify, at the outcrop scale, the different deformation phases that affected the rocks observed. Tectonic structures have been identified and described basing on the knowledge acquired in structural geology. From this description, a kinematic and dynamic analysis of deformations was made. Then during this stage, photographs of the main lithologies and structures were taken. Finally, detailed structural maps by sectors were designed to assess the path of each deformation that affected the study site and the distribution of structures. These maps were produced by geolocating tectonic structures using GPS.

3.2. Microscopic and Microstructural Petrography

For a thorough understanding of the petrographic and structural characteristics and for metamorphic characterization, six (6) thin sections were designed from paragneiss samples collected in the field (**Table 1**). These thin sections were studied at the laboratory of Geology and Metallogeny at the Félix Houphouët-Boigny

Table 1. Inventory of samples collected and thin sections designed.

Identifiers	Structures Lithologie sampled	UTM Coordinates	D°M'S" Coordinates	Number of thin section	Code of thin section
C1	Migmatitic Paragneiss (neosome)	29N 730,764 513,398	4°38'25.6" 6°55'16.6"	1	C1PV
C2	Migmatitic Paragneiss	29N 730,792 513,431	4°38'26,5" 6°55'15,7"	0	
C3	Crenulation (Migmatitic Paragneiss)	29N 730,815 513,466	4°38'27.8" 6°55'15"	0	
C4	Shear Corridor (Foliation)	29N 730,835 513,482	4°38'28.3" 6°55'14.3"	0	
C5	Microfolds (Migmatitic Paragneiss)	29N 730,825 513,487	4°38'28.5” 6°55’14.6”	1	C5PH
C6	Shear Corridor (Foliation)	29N 730,814 513,488	4°38'28.5" 6°55'15"	1	C6PH
C7	Crenulation (Migmatitic Paragneiss)	29N 730,830 513,471	4°38'28" 6°55'14.5"	1	C7PH
C8	Crenulation (Migmatitic Paragneiss)	29N 730,821 513,445	4°38'27.1" 6°55'14.8"	1	C8PV
C9	Foliation Migmatitic Paragneiss (paleosome)	29N 730,835 513,477	4°38'28.2" 6°55'14.3"	1	C9PH

University, using a polarizing optical microscope surmounted by a camera, all connected to a computer. The microscopic petrography consisted in the description of the texture and mineralogical composition of the C1PV and C9PH sections designed in the different parts of the paragneisses. The minerals were identified on the basis of their optical properties in natural and polarized light. The micro-structural work consisted in describing the structures at the scale of the thin slide and associating the mineralogical parageneses with the deformation phases and episodes. Indeed, a distinction of minerals based on the general chronological criteria of mineral crystallization and specific to metamorphic rocks has been made. Thus, were identified in relation to each phase and episode of deformation, the ante-kinetic, synkinematic minerals defining the paragenesis and post-kinematic minerals. This made it possible to establish the evolution of metamorphism according to the deformations.

4. Results

4.1. Petrographic Characteristics

The macroscopic and microscopic observation of the geological formations of Grand-Béréby, especially those of the coconut grove of the Hotel Complex, has made it possible to identify migmatitic paragneisses.

These migmatitic paragneisses appear as a close association between metamorphic and melted parts (**Figure 2**). The metamorphic part, called the paleosome, is the finely ribboned foliated zone: it is the gneiss zone in where the paragneiss characters persist. This part shows garnet intercalations in the dark bands (**Figure 2(b)**). In thin sections, it has a granolepidoblastic texture with a pronounced alternation of light and dark levels (**Figure 2(c)**). The bright levels are rich in quartz and feldspar (**Figure 2(d)**). Myrmekite, microcline, plagioclase and cordierite with bevelled macles are found therein. Biotite and fibrous sillimanite are abundant in the levels. This abundance of quartzo-feldspathic elements, biotite and alumina silicate testifies to the para-derived origin of these gneisses.

The molten part called the neosome, is made up of leucosome or mobilizate and melanosome or restites (**Figure 2(a)**). The leucosome is either in the form of folded bright patches (**Figure 2(a)**), with aplite and most often pegmatite mineralogy; or as patches with a grained and micrograined texture (**Figure 2(b)**). These secondary lithologies are evidence of partial fusion or anatexis of the paragneiss. As for the melanosome, it corresponds, within the neosome, to refractory residues (**Figure 2(b)**) which are concentrations of biotite and a fibrous whitish, lamellar, pearly-looking mineral of various sizes, sillimanite. In thin sections, the neosome has a granolepidoblastic texture with alternating bright and dark levels very weakly expressed (**Figure 2(e)**). Its mineralogical composition is identical to that of the paleosome.

4.2. Structural Characteristics

On our study site, depending on the deformation mechanism, the structures

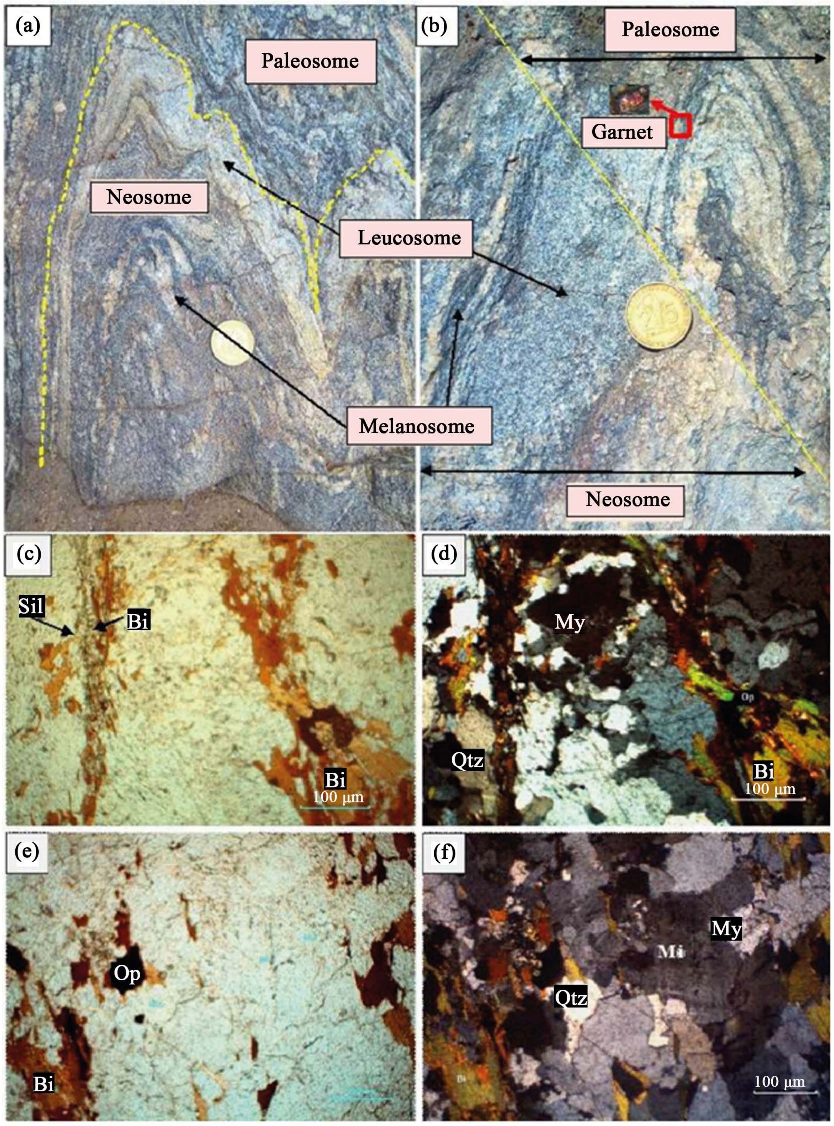

Figure 2. Macroscopic and microscopic aspect of migmatitic paragneisses. (a) Folded leucosome; (b) Leucosome and garnet in a dark level of paragneiss, (c) Paleosome; (e) Neosome. (c)-(e) Natural light; (d)-(f) Polarized light.

observed can be distributed into two groups, namely plastic or ductile deformation structures and brittle or fragile deformation structures.

4.2.1. Ductile Deformation Structures

1) Foliation

The foliations observed in the gneissic part of the migmatite present two different characteristics with regard to their configuration, especially with regard to direction and dip:

- The foliation (S1), whose plane is measured (N140˚, 30˚NE), is characterized by alternating bright and dark levels of varying thickness and folding (Figure 3(a)) and most often recrystallized. It shows evidence of an earlier NE-SW flattening with a vertical component of the original rock stratification.

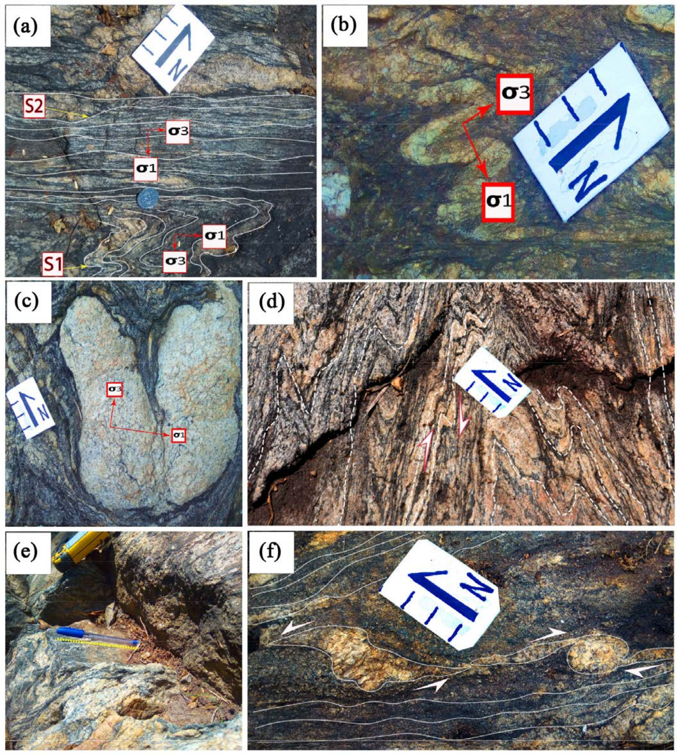

Figure 3. Macroscopic appearance of ductile deformation structures. (a) S1 et S2 foliations; (b) Ptymatic folds; (c) Flattened concentric fold; (d) Asymmetrical Z folds; (e) Plunging axis folds; (f) Sigmoid figure and winding structure.

- The foliation (S2) has a N50˚-oriented plane with a subvertical dip (Figure 3(a)). It is characterized by an alternation of dark levels and fine, straight and bright levels followed by a mineral stretching lineation. This foliation is due to a second NW-SE flattening which caused the transposition of the foliation (S1) into N50˚-oriented Shear.

2) Folds

The folds observed at the study site have different characteristics, which means that they are put in place through different mechanisms.

- Ptymatic folds: with an axial plane parallel to foliation N50˚ (S2), these are tight folds with regular and rounded hinges (Figure 3(b)). These folds result from a buckling mechanism (pure bending with N140˚-oriented $\sigma 1$), small pegmatite veins developed within a matrix with a very high viscosity contrast.
- Flattened concentric fold: its axial plane is at N50˚. This fold combines the effects of a first mode of deformation (NW-SE bending of the layers) and those of the second mode (N50˚ flattening), which are manifested by the stretching of the flanks (curled flanks) and the thickening of the hinges (Figure 3(c)).
- Asymmetrical Z folds: these are secondary folds that form in the flanks of large folds having an axial plane parallel to the N50˚ foliation (S2) (Figure 3(d)). They can also be found near sinistral asymmetric boudins. They reveal an N50˚ dextral shear episode posterior to bending (NW-SE).

- Similar folds with plunging axis: the axis of these folds has the following characteristics (N50˚, 30˚NE), the axial plane is N50˚-oriented and hangs subvertically (**Figure 3(e)**).

These folds are the result a NW-SE crushing consisting of a N140˚-oriented (NW-SE) bending with main stress ($\sigma 1$), followed by a simple shear. The total absence of vertical motion markers near these folds suggests that the plunging of the axis is due to a layer inclination (S0) caused by an oblique bedding before folding.

3) Boudins

The observed boudins have an axis oriented in parallel with the N50˚-oriented foliation. Both symmetric and asymmetric boudins can be found. Symmetric boudins: they are lenticular in shape. They are the result of a pinch-swelling process due to an intense and essentially coaxial deformation, especially traction. This traction causes the fragments to shift as a result of an N50˚ extension. Asymmetric boudins: they have a sigmoidal shape and are sandwiched between two thin dextral shear lanes, materialized by the asymmetric Z folds and dextral winding structures juxtaposed to them in the N50˚ direction (**Figure 3(f)**). The asymmetry of their shape translates a N50˚ sinistral shear of pinch-swelling structure. This shear is post-boudinage and antithetic to the general shear which is dextral.

4.2.2. Brittle Deformation Structures

1) Fracture Schistosity

An N140˚-oriented fracture schistosity (parallel to the first generation of foliation in the migmatitic paragneiss) and subvertical dip schistosity are observed. This schistosity affects both migmatitic paragneisses and pegmatites (**Figure 4**). It cuts these rocks into vertical sheets (microlithons), evenly spaced and about ten centimeters thick. This deformation would be contemporary to the opening of the Atlantic Sea.

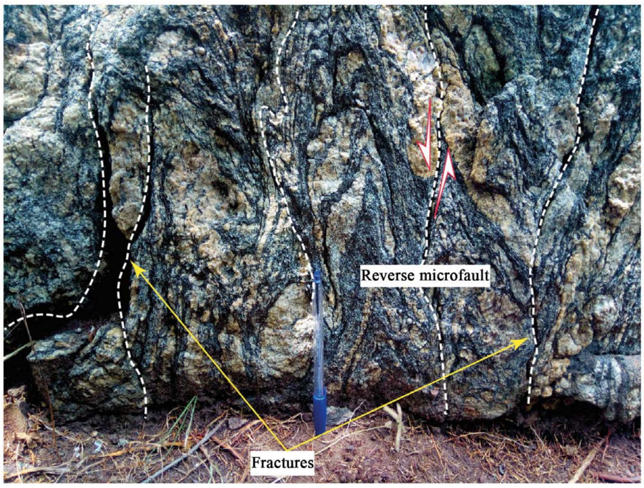

Figure 4. Macroscopic appearance of brittle deformation structures. Fracture Schistosity and fold-fracture schistosity.

2) Fold-fracture schistosity

A fold-fracture schistosity whose plane is parallel to N50˚ foliation and subvertical was observed in the migmatitic paragneiss. In this deformation, reverse microfaults are associated with microfolding. The axial plane of the decimetrically similar microfolds is N50˚ oriented and their flanks are stretched to the extreme along spaced schistosity surfaces interposed between successive hinges. This stretching eventually fractures these flanks, creating ductile fractures and reverse faults (**Figure 4**). This process cuts the rock into thick sheets (the size of those of the fracture schistosity) that are more or less orthogonal to the average arrangement of the folded beds (**Figure 4**). This mechanism is the result of an increased crushing associated with NW-SE folding.

4.2.3. Structural Distribution

Depending on the scale and occurrence of the structures, the structural distribution has been defined on three sectors, namely sector 1, 2 and 3. This distribution accounts for three deformation phases. These are phases D1, D2 and D3. Phase D1 is a subvertical NE-SW flattening marked by the N140˚ foliation visible in all sectors. The second phase, D2, is a progressive ductile deformation consisting of three ductile deformation episodes in a well-defined chronological order. This is the first episode which is a NW-SE bending affecting the N140˚ foliation. This bending is materialized by the ptymatic folds and flattened concentric folds visible in sector 1 (**Figure 5(a)**). This bending is followed by the second episode of D2, which is an NW-SE pure shear (flattening) materialized by the N50˚ foliation visible in all sectors and the symmetric boudins visible in the sector 1. This flattening is followed in turn by the third episode, which is a

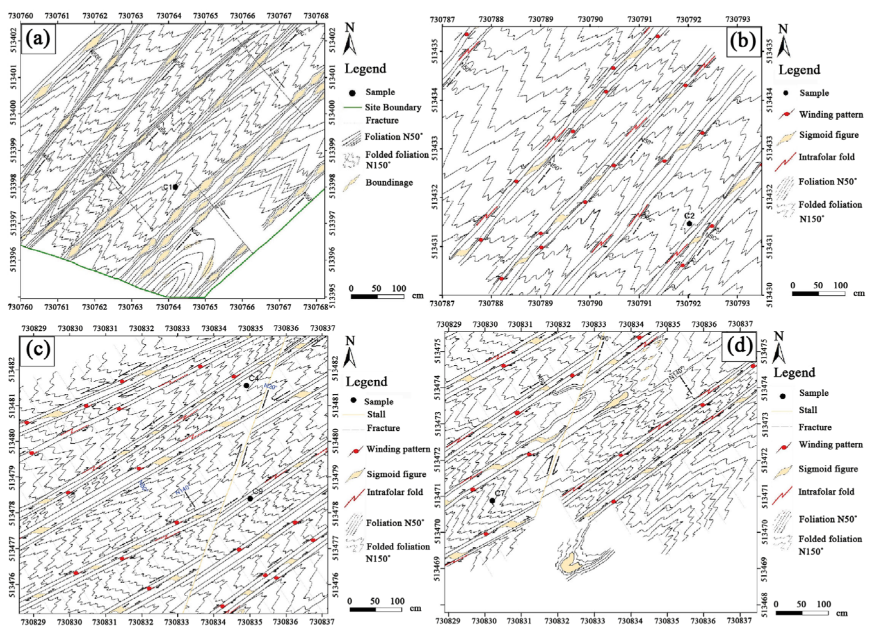

Figure 5. Structural distribution on site. (a) Structural map on sector 1; (b) Structural map on sector 2; (c) Structural map on sector 3 (North); (d) Structural map on sector 3 (South).

simple shear event materialized by N50˚-oriented dextral shear planes visible in sector 2 (Figure 5(b)) and sector 3 (Figure 5(c), Figure 5(d)). In these shear planes are located sigmoid figures, winding structures and asymmetrical folds. The third phase D3, is a brittle deformation due to NE-SW compression, materialized by an N140˚-oriented fracture schistosity visible in sector 3 (Figure 5(c), Figure 5(d)).

4.3. Microstructural and Metamorphic Characteristics

The characterization of the metamorphism that prevailed during the various deformation phases and episodes described, required a microstructural analysis that is an essential complement to the geometrical and kinematic study of the deformations. In the framework of our study, we will perform a microstructural analysis of five (5) thin sections made from samples taken from the identified deformation structures.

4.3.1. C8PV, C5PH and C7PH Thin Sections

The study of the C8PV, C5PH and C7PH thin sections designed at the level of the crenulations of samples C8, C5 and C7, revealed two (2) microstructures, namely a foliation and the microfolds formed by it (Figure 6(a)). This foliation is marked by alternating bright quartzo-feldspathic levels and dark levels rich in biotite and sillimanite.

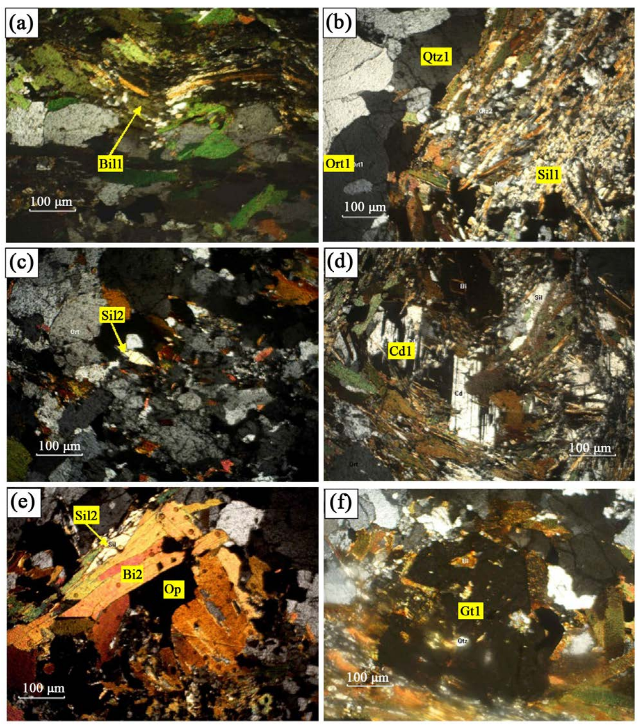

Figure 6. Microstructural observation of C8PV, C5PH, C7PH thin sections. (a)-(e) Thin section C8PV; (b)-(d) Thin section C5PH; (c)-(f) Thin section C7PH. (a) Folded dark levels; (b)-(d)-(e) Hinge and microfold flanks. (Qtz: quartz, Ort: orthose, Bi: biotite, Sil: sillimanite, Op: opaque minéral, Cd: cordiérite, Gt: garnet). 1, 2, 3 = first generation, second generation, third generation.

The study of these thin sections also revealed the synkinematic minerals defining the parageneses associated with the D1 phase (the NE-SW subvertical flattening) and the first episode of the D2 phase (the NW-SE bending). The synkinematic minerals defining the paragenesis associated with the D1 phase are biotite 1 (Bi1), sillimanite 1 (Sil1) and cordierite 1 (Cd1). Biotite 1 is folded and is located at the hinges of the microfolds (Figure 6(a)). Sillimanite 1 has a destabilized appearance (Figure 6(b)) at the hinges. Cordierite 1 (Cd1) is cut by some sillimanites and biotite (Figure 6(d)). This paragenesis reflects a low-grade syntectonic metamorphism in the amphibolite facies.

The synkinematic minerals defining the paragenesis associated with the first episode of D2 (the NW-SE bending) are quartz 2 (Qtz2), orthose 2 (Ort2), sillimanite 2 (sil2), biotite 2 (Bi2) and garnet (Gt1). Quartz 2 and orthose 2 are elongated in parallel with the flanks of the microfolds (Figure 6(b)). Sillimanites 2 are prismatic (Figure 6(c)). Biotites 2 are located at the hinges and form polygonal arcs (Figure 6(e)). The garnets 1 are subautomorphic, rounded and poeciloblastic garnets containing inclusions of quartz, sillimanite and biotite (Figure 6(f)). This paragenesis is typical of a medium-grade syntectonic metamorphism in the amphibolite facies.

4.3.2. C9PH and C6PH Thin Sections

The study of the C9PH and C6PH sections, designed at the level of the shear zone, revealed the synkinematic minerals defining the paragenesis associated with the last episodes of the D2 phase, i.e. the pure shear NW-SE and the simple shear N50˚. The synkinematic minerals relative to pure shear NW-SE are garnet (Gt2), biotite (Bi3), sillimanite (Sil3), quartz (Qtz3) and orthose (Ort3). These minerals have a particular habit and are described as follows:

- Garnet (Gt2): these are garnets stretched and elongated in parallel with foliation N50˚ (Figure 7(a)). In these garnets, the mineral inclusions are also elongated and highlight an internal foliation (Si) which runs parallel to the external foliation (Se) of the matrix (Figure 7(a)). The parallelism of these inclusions suggests a synkinematic growth of these garnets, compared to the pure shear NW-SE.
- Biotite (Bi3): these are biotites oriented in parallel with the N50˚ foliation (S2) (Figure 7(b)). This foliation in line with the orientation suggests a synkinematic growth of these biotites with respect to the pure shear NW-SE.
- Sillimanite (Sil3): these are, like biotite (Bi3), elongated in the plane of the N50˚ foliation (Figure 7(b)).
- Quartz (Qtz3): it is in the form of very thin ribbons, oriented in parallel with the N50˚ foliation (Figure 7(b)).

This paragenesis indicates a high-grade syntectonic metamorphism in the granulite facies.

The synkinematic minerals with respect to the simple shear N50˚ are cordierite 2 (Cd2), biotite 4 (Bi4), sillimanite 4 (Sil4) and quartz 4 (Qtz4). These minerals have a particular habit and are described as follows:

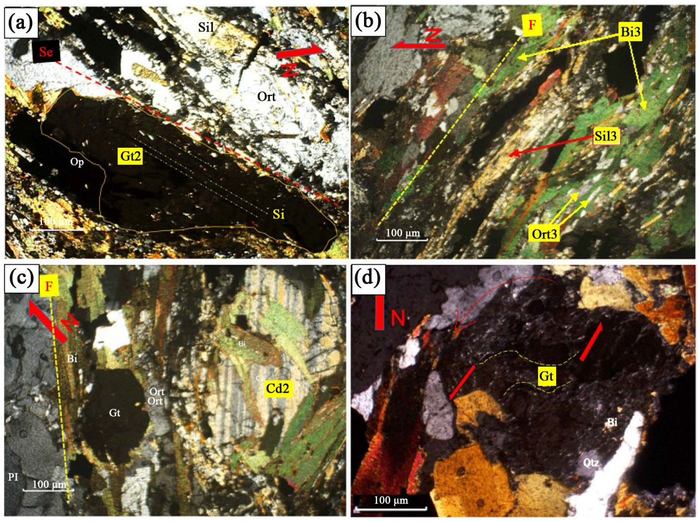

Figure 7. Microstructural observation of C9PH and C6PH thin sections. (a)-(c)-(d) Thin section C6PH; (b) Thin section C9PH. (Qtz: quartz, Bi: biotite, Sil: sillimanite, Op: opaque mineral, Cd: cordiérite, Gt: grenat, F: foliation trend, Si: internal foliation, Se: external foliation). 2, 3 = second generation, third generation.

- Cordierite (Cd2): these are oriented in parallel with the direction of the simple shear N50˚ with biotite inclusions oriented obliquely to the N50˚ foliation (**Figure 7(c)**).
- Biotite 4 (Bi4), sillimanite 4 (Sil4) and quartz 4 (Qtz4): they form in helical garnet destabilized and cracked by their rotation due to the sinistral shear N50˚ (**Figure 7(d)**).

This paragenesis indicates a medium-grade syntectonic metamorphism in the amphibolite facies.

5. Discussion

The gneisses of this Gbowé sector have a granolepidoblastic texture and are of sedimentary origin revealed by the mineralogical assemblage marked by an abundance of quartzo-feldspathic elements (quartz, plagioclase, myrmekite, microcline), biotite, cordierite, and sillimanite. These results corroborate those of Kouadio et al. (2016) and Kouadio (2017) who identified paragneisses in the sector of Grand-Béré by using a petrographic and geochemical approach. These paragneisses are characterized by an absence of muscovite, unlike those identified by Bard & Lemoine (1976), which contain muscovite and staurotide in addition to garnet and biotite (Koffi et al., 2018). In addition, the paragneisses in our study area present a migmatitic character due to the onset of anatexis. This is illustrated macroscopically by the duality between neosome and paleosome, and on thin slide by the abundance of myrmekite and the disappearance of the alternation between micaceous and quartzo-feldspathic levels (Koffi et al., 2018). The migmatitic character of the gneisses of the SASCA domain was also highlighted by Kouamelan (1996), particularly for Monogaga and Balmer orthogneisses (Kouamelan et al., 2015). Moreover, according to Papon (1973) a paragenesis composed of biotite + garnet + cordierite + sillimanite shows an intensity of metamorphism sufficient to allow anatexis.

From a structural point of view, the tectonics described (D1, D2, D3) have the characteristics of the Eburnean megacycle. Our assertions corroborate those of Kouadio (2017) who identified the last two episodes of Phase D2. However, he considers them as two distinct phases D2 and D3 deformation. This tectonics differs from that described by Bard & Lemoine (1976) at Monogaga and Kounoukou, which indicates a superposition of four folding phases. The D3 phase of brittle deformation corroborates the assertions of Vidal & Alric, (1994) according to which the last tectonic events to have marked the Birimian are post-Birimian movements such as the N130˚ fractures.

The microstructural study allowed us to follow the polymorphic evolution during the phases and episodes of flexible deformation and to specify the succession between a prograde metamorphism from amphibolite to granulite facies and a retrograde metamorphism from granulite to amphibolite facies (Pitra et al., 2010). This retromorphosis was also highlighted by Kouadio (2017). According to this author, the migmatitic paragneisses in the study area were affected by a transitional metamorphism going from medium-grade sub-solidus amphibolite facies to low-grade amphibolite facies via supra-solidus granulite facies.

6. General Conclusion

This study enabled us to highlight the petrographic, structural and metamorphic characteristics of the Grand-Béréby paragneisses in the South-West of Côte d'Ivoire (Coconut grove sector of the Hotel Complex). On the petrographic level, we have highlighted migmatitic paragneisses, which contains several minerals (quartz, plagioclase, biotite, garnet, myrmekite, microcline, cordierite and sillimanite). From a structural point of view, we can note three deformation phases, especially phases D1, D2 and D3, materialized by characteristic planar structures. D1 is an NE-SW subvertical flattening. It is manifested by an NW-SE foliation (S0 - 1) in parallel with the stratification (S0) and by the near absence of stretching lineation. D2 is a progressive ductile deformation composed of three ordered episodes of deformation. It begins with an NW-SE bending episode which results in ptymatic folds and concentric folds with an N50˚-oriented subvertical axial plane. This bending is generalized to give pure shear in the same direction. This pure shear is manifested by a N50˚ oriented foliation (S2) and symmetric boudins. It intensifies in turn to give a simple dextral shear N50˚ which is materialized by structures oriented in parallel with the S2. These are small shear planes in which intrafoliate folds, dextral winding figures, and sinistral antithetic and sigmoid figures are found. Phase D2 would be due to an NW-SE to NNW-SS compression. D3 is a brittle tectonics materialized by a fracture schistosity with N140˚-oriented and subvertical planes.

On the microstructural and metamorphic level, we can note a polymetamorphism generated by the phases of flexible deformation. The polymetamorphic evolution took place through a succession between a prograde metamorphism from amphibolite to granulite facies during the transition between D1 and D2; and a retrograde metamorphism from granulite facies (at Gt + Pl + Bi + Sil + Qtz) to amphibolite facies (at Gt + Pl + Bi + Sil + Cd + Qtz). This generalized retroromorphosis in all formations occurred during D2.

Conflicts of Interest

The authors declare no conflicts of interest regarding the publication of this paper.

References

Arnould, M. (1961). *Geological Studies of Precambrian Migmatites and Granites of Northeastern Côte d'Ivoire and Southern Upper Volta* (174 p.). BRGM Memory, France.

Bard, J. P., & Lemoine, S. (1976). Superimposed Tectonic Phases in the Precambrian Metasediments of the Western Coastal Domain of Côte d'Ivoire. *Precambrian Research, 3,* 209-229. https://doi.org/10.1016/0301-9268(76)90009-7

Blarez, E. (1986). *The Continental Margin of Côte d'Ivoire-Ghana. Structure and Evolution of a Transforming Continental Margin* (188 p). PhD, Paris: University Paris VI.

Boher, M., Abouchami, W., Michard, A., Albarède, F., & Arndt, N. T. (1992). Crustal Growth in West Africa at 2.1 Ga. *Journal of Geophysical Research, 97,* 345-369. https://doi.org/10.1029/91JB01640

Bonhomme, M. (1962). *Contribution to the Geochronological Study of the West African Shelf* (62 p.). PhD, Clermont-Ferrand: Ann. Fac. Univ. Sc., 5.

Camil, J. (1984). *Petrography, Chronology of the Archean Granulitic Ensembles and Associated Formations of the Man Region (Ivory Coast). Implications for the Geological History of the West African Craton* (306 p.). State Thesis, Abidjan: University of Abidjan.

Doumbia, S. (1998). *Geochemistry, Geochronology and Structural Geology of the Birimian Formations of Katiola—Marabadiassa. Magmatic Evolution and Geodynamic Context of the Paleoproterozoic* (251 p). PhD Thesis, Orléans: University of Orleans.

Gasquet, D., Barbey, P., Adou, M., & Paquette, J. L. (2003). Structure, Sr-Nd Isotope Geochemistry and Zircon U-Pb Geochronology of the Granitoids of Dabakala Area (Côte d'Ivoire): Evidence for a 2.3 Ga Crustal Growth Event in the Palaeoproterozoic of West Africa? *Precambrian Research, 127,* 329-354. https://doi.org/10.1016/S0301-9268(03)00209-2

Koffi, G. R.-S., Kouamelan, A. N., Allialy, M. E., Coulibaly, Y., & Peucat, J.-J. (2020). Re-Evaluation of Leonian and Liberian Events in the Geodynamical Evolution of the Man-Leo Shield (West African Craton). *Precambrian Research, 338,* Article ID: 105582. https://doi.org/10.1016/j.precamres.2019.105582

Koffi, Y. A., Kouamelan, A. N., Djro, S. C., Kouadio, F. J.-L. H., Teha, K. R., Kouassi, B. R., & Koffi, G. R. S. (2018). Petrography and Origin of the Metasediments of SASCA Domain (SW of Côte d'Ivoire). *International Journal of Innovation and Applied Studies, 23,* 451-464. http://www.ijias.issr-journals.org

Kouadio, F. J. L. H. (2017). *Petrostructural Study of the Geological Formations of the South-West of Côte d'Ivoire (Bliéron Grand-Béréby Sector): Contribution of Geochemistry and Coupled Deformation-Metamorphism* (220 p.). Thesis Unique, Cocody: Félix Houphouët-Boigny University of Cocody.

Kouadio, F. J.-L. H., Djro, S. C., Kouamelan, A. N., Allialy, M. E., & Koffi, Y. A. (2016). Petrographic and Geochemical Signatures of the Paragneisses of the Tabou and Grand-Béréby Sectors (South-Western Côte d'Ivoire). *International Journal of Innovation and Applied Studies, 18,* 646-658. http://www.ijias.issr-journals.org

Kouamelan, A. N. (1996). *Geochronology and Geochemistry of the Archean and Proterozoic Formations of the Man Ridge in Côte d'Ivoire Implications for the Archean-Protérozoïque* (p. 290). Thèse de Doctorat Université de Rennes1, France, No. 73.

Kouamelan, A. N., Djro, S. C., Allialy, M. E., Piquette, J.-L., & Peucat, J.-J. (2015). The Oldest Rock of Ivory Coast. *Journal of African Earth Sciences, 103,* 65-70. https://doi.org/10.1016/j.jafrearsci.2014.12.004

Kouamelan, A. N., Kra, K. S. A., Djro, S. C., Paquette, J.-L., & Peucat, J.-J. (2018). The Logoualé Band: A Large Archean Crustal Block in the Kenema-Man Domain (Man-Leo Rise, West African Craton) Remobilized during Eburnean Orogeny (2.05 Ga). *Journal of African Earth Sciences, 148,* 6-13. https://doi.org/10.1016/j.jafrearsci.2017.09.004

Kouamelan, A. N., Peucat, J. J., & Delor, C. (1997a). Reliques archéennes (3.15 Ga) au sein du magmatisme Birimien (2.1 Ga) de Côte d'Ivoire, Craton Ouest-Africain. *Comptes Rendus de l'Académie des Sciences, 324,* 719-727.

Kouamelan, A. N., Peucat, J. J., & Delor, C. (1997b). Geochronological Evidence for Reworking of Archean Terrains during the Early Proterozoic (2.1 Ga) in the Western Côte d'Ivoire (Man Rise—West African Craton). *Precambrian Research, 86,* 177-199. https://doi.org/10.1016/S0301-9268(97)00043-0

Milesi, J. P., Feybesse, J. L., Pinna, P., Deschamps, Y., Kampunzu, H., Muhongo, S., Lescuyer, J. L., Le Goff, E., Delor, C., Billa, M., Ralay, F., & Heinry, C. (2004). Geological Map of Africa 1:10,000,000, SIG Afrique Project. In *20th Conference of African Geology*. Orleans: BRGM.

Papon, A. (1973). *Geology and Mineralization of Southwestern Côte d'Ivoire* (284 p.). Memory of the BRGM, Paris, No. 80.

Petersson, A., Scherstén, A., & Gerdes, A. (2017). Extensive Reworking of Archaean Crust within the Birimian Terrane in Ghana as Revealed by Combined Zircon U-Pb and Lu-Hf Isotopes. *Geoscience Frontiers, 9,* 173-189. https://doi.org/10.1016/j.gsf.2017.02.006

Petersson, A., Scherstén, A., Kemp, A. I. S., Kristinsdóttir, B., Kalvig, P., & Annum, S. (2016). Zircon U-Pb-Hf Evidence for Subduction Related Crustal Growth and Reworking of Archaean Crust within the Palaeoproterozoic Birimian Terrane, West African Craton, SE Ghana. *Precambrian Research, 275,* 286-309. https://doi.org/10.1016/j.precamres.2016.01.006

Pitra, P., Kouamelan, A., Ballevre, M., & Peucat, J.-J. (2010). Palaeoproterozoic High-Pressure Granulite Overprint of the Archean Continental Crust: Evidence for Homogeneous Crustal Thickening (Man Rise, Ivory Coast). *Journal of Metamorphic Geology, 28,* 41-58. https://doi.org/10.1111/j.1525-1314.2009.00852.x

Pouclet, A., Doumbia, S., & Vidal, M. (2006). Geodynamic Setting of the Birimian Volcanism in Central Ivory Coast (Western Africa) and Its Place in the Palaeoproterozoic Evolution of the Man Shield. *Bulletin de la Societe Geologique de France, 177,* 105-121. https://doi.org/10.2113/gssgfbull.177.2.105

Thieblemont, D., Goujou, J. C., Egal, E., Cocherie, A., Delor, C., Lafon, J. M., & Fanning, C. M. (2004). Archaean Evolution of the Leo Rise and Its Eburnean Reworking. *Journal of African Earth Sciences, 39,* 97-104. https://doi.org/10.1016/j.jafrearsci.2004.07.059

Vidal, M., & Alric, G. (1994). The Palaeoproterozoic (Birimian) of Haute-Comoé in the West African Craton, Ivory Cost: A Transtensional Back-Arc Basin. *Précambrian Re-*

search, 65, 207-229. https://doi.org/10.1016/0301-9268(94)90106-6

Vidal, M., Gumiaux, C., Cagnard, F., Pouclet, A., Ouattara, G., & Pichon, M. (2009). Evolution of a Paleoproterozoic "Weak Type" Orogeny in the West African Craton (Côte d'Ivoire). *Tectonophysics, 477,* 145-159. https://doi.org/10.1016/j.tecto.2009.02.010